Polyhedron 247 (2024) 116729

Contents lists available at ScienceDirect

Polyhedron

journal homepage: www.elsevier.com/locate/poly

Towards an efficient oxidation of sulfides to sulfoxides over magnetic and grafted polyoxometalate on graphene oxide nanosheets

Masoume Malmir [a,1], Majid M. Heravi [a,2,*], Zahra Yekke-Ghasemi [a], Masoud Mirzaei [b,c,3,*]

[a] Department of Organic Chemistry, Faculty of Chemistry, Alzahra University, Tehran, Iran
[b] Department of Chemistry, Faculty of Science, Ferdowsi University of Mashhad, Mashhad 9177948974, Iran
[c] Khorasan Science and Technology Park (KSTP), 12th km of Mashhad-Quchan Road, Mashhad 9185173911, Khorasan Razavi, Iran

ARTICLE INFO

Keywords:
Keggin
Graphene oxide
Oxidation process
Sulfides
Sulfoxides

ABSTRACT

In this study, a tri-component composite consisting of Fe_3O_4 nanoparticles, Keggin-type polyoxometalate, and graphene oxide components was prepared using an ultrasonic-assisted method. The resulting $Fe_3O_4/SiW_{12}/GO$ composite was successfully characterized using multiple methods. The performance of the $Fe_3O_4/SiW_{12}/GO$ composite as a heterogeneous catalyst for the oxidation of sulfides to sulfoxides was investigated under mild conditions, with H_2O_2 serving as the oxidant. The catalyst exhibited excellent stability and high yields, completing the conversions within one hour. Furthermore, the $Fe_3O_4/SiW_{12}/GO$ catalyst demonstrated remarkable recyclability, as it could be recovered and reused up to four times without any significant loss in activity. This finding was supported by the results obtained from the ICP-OES analysis, which confirmed the negligible leaching of the active site. One of the key advantages of the $Fe_3O_4/SiW_{12}/GO$ catalyst is its heterogeneous nature, which allows for its rapid recovery from the reaction mixture. Additionally, it offers smooth and clean reaction conditions at room temperature, making it an innovative and cost-effective choice for accelerating reaction times. In summary, the $Fe_3O_4/SiW_{12}/GO$ composite represents a highly efficient and versatile heterogeneous catalyst with a unique structure. Its exceptional stability, high yields, and recyclability make it a superior choice for various organic–inorganic hybrid catalytic reactions conducted under mild conditions.

1. Introduction

Polyoxometalates (POMs) are a remarkable class of inorganic materials with redox activity. They consist of metal-oxide ions connected by bridge oxygen atoms, forming clusters ranging in size from nanometers to micrometers. POMs have versatile structures and find applications in various fields such as catalysis [1], sorption [2], sensing [3], magnetism [4], medicine [5], and batteries [6]. The catalytic activity of POMs, coupled with their stable redox states, enables them to act as electron reservoirs, resulting in the formation of mixed valence state species. However, the solubility of POMs in different solvents limits their recyclability and reusability in homogeneous catalysis. To address this issue and align with the principles of green chemistry, researchers have developed POM-based composites where POMs are immobilized on suitable supports like carbon nanomaterials (CNMs) [7].

Graphene oxide (GO), characterized by its well-organized sheet structures, belongs to the category of microporous carbon nanomaterials. Its exceptional properties, including high mechanical strength and surface area, make GO an excellent candidate for catalytic applications [8]. Moreover, GO is employed as a support material to overcome the limitations associated with POM-based catalysts, such as solubility and low surface area. Notably, the incorporation of magnetic Fe_3O_4 nanoparticles onto GO enhances the composite's utility in various fields, including environmental applications and catalysis, owing to its desirable magnetic property, which facilitates easy removal from the reaction mixture [9].

Sulfoxide moieties play a crucial role as powerful synthetic intermediates and motifs in the production of biological and chemical

* Corresponding authors at: Department of Organic Chemistry, Faculty of Chemistry, Alzahra University, Tehran, Iran and Department of Chemistry, Faculty of Science, Ferdowsi University of Mashhad, Mashhad 9177948974, Iran.
E-mail addresses: m.malmir@alzahra.ac.ir (M. Malmir), mmheravi@alzahra.ac.ir (M.M. Heravi), mirzaeesh@um.ac.ir (M. Mirzaei).
[1] ORCID: 0000-0003-1537-8076.
[2] ORCID: 0000-0002-9259-0591.
[3] ORCID: 0000-0002-7256-4601.

https://doi.org/10.1016/j.poly.2023.116729
Received 13 August 2023; Accepted 4 November 2023
Available online 4 November 2023

products. Traditional sulfide oxidation methods require stoichiometric amounts of organic or inorganic oxidizing agents, posing safety risks and generating substantial amounts of toxic waste. In recent years, there has been a growing interest in developing selective catalytic oxidation methods using green oxidants [10]. Dilute hydrogen peroxide has emerged as a promising option due to its non-toxic nature, affordability, and effectiveness as an oxidizing reagent [11]. Additionally, the oxidation reaction using hydrogen peroxide offers greater control compared to molecular oxygen and air.

In recent years, there has been a growing interest in the development of catalysts containing transition metals incorporated into a framework or grafted onto solid surfaces for various oxidation reactions using H_2O_2 as an oxidant [12–21]. Iron-based complexes have particularly gained attention due to their low cost and low toxicity, making them suitable for homogeneous catalysis. However, one major drawback of these catalysts is the difficulty in separating them from the reaction mixture. A recent study by Liang-Nian and coworkers [22] demonstrated the effective use of $Fe(acac)_2$ for the selective oxidation of sulfides to sulfoxides using oxygen in polyethylene glycol as a solvent. Although this approach showed promising results, there is still a need for metal-containing catalysts, such as magnetic catalysts [21,23], that can simplify the recovery process and enhance reaction efficiency. In 2022, Moini and coworkers reported a novel method for the oxidation of sulfides using magnetic nanoparticles, highlighting their potential in waste reduction, catalyst recovery, and avoidance of allylic oxidation products formation [24]. Furthermore, GO have also been recognized for their unique surface properties and ability to oxidize sulfides with excellent conversion rates, as reported by Abdi and coworkers [25]. Based on these recent findings [26,27], there is a pressing need to develop a new, clean, and environmentally friendly method that can overcome the limitations of previous approaches. Overall, the development of POM-based catalysts, supported by GO and magnetic nanoparticles, could represent a significant advancement in the field of oxidation reactions.

In line with our ongoing efforts to introduce heterogeneous catalysts [28–41], particularly focusing on POM-based catalysts [1,42,43] and leveraging the synergistic effects and advantages offered by POMs, Fe_3O_4 nanoparticles and GO, we present here the design of a tri-component composite ($Fe_3O_4/SiW_{12}/GO$) comprising Keggin-type POM clusters with an oxygen-enriched surface and magnetic GO with a high surface area (Fig. 1). The $Fe_3O_4/SiW_{12}/GO$ composite demonstrates promising catalytic performance as a magnetic catalyst for the oxidation of sulfides to sulfoxides using peroxide. As anticipated, $Fe_3O_4/SiW_{12}/GO$ functions simultaneously as a Lewis acid/base, thereby enhancing the catalytic activity through the incorporation of Fe_3O_4 onto the GO support (Fig. 1). Furthermore, we investigate the recyclability of $Fe_3O_4/SiW_{12}/GO$ to assess the nature and stability of the catalyst. These innovative approaches effectively address the challenges associated with recyclability, reusability, and waste generation, aligning with the principles of green chemistry and promoting sustainable practices within the chemical industries.

2. Methods

2.1. Chemicals and materials

All chemicals were purchased from Merck (Darmstadt, Germany, https://www.merckmillipore.com) and Sigma-Aldrich (St. Louis, MO, USA, https://www.sigmaaldrich.com) and used without crystallization or purification. To conduct oxidation, sulfides, H_2O_2, methanol, ethanol, acetonitrile, and deionized water were used.

2.2. Instrumentation

Also, the infrared spectra of the catalysts were recorded in the range of 4000–400 cm^{-1} on a Thermo Nicolet/AVATAR 370 Fourier transform spectrophotometer using the KBr discs. Powder XRD patterns were obtained using a PANalytical B.V. diffractometer with Cu Kα radiation ($\lambda = 1.54184$ Å) at room temperature with the scan range $2\theta = 5$ to 50° and step size of 0.05 °C and step time of 1 s. The catalyst morphology was studied by scanning electron microscopy (SEM) using a Leo 1450 VP, Germany instrument. The energy-dispersive X-ray (EDX) is performed using LEO-1450 VP at an acceleration voltage of 10.00 kV and resolution of about 500 nm (Zeiss, Germany). Magnetic measurements were carried out by means of the vibrating sample magnetometer (VSM) at room temperature (300 K). Adsorption studies were performed using a isotherm surface area analyzer from Micromeritics Instrument Corporation with N_2 at 77 K. Metal content was measured by the Spectro Arcos ICP-OES spectrometer model 76,004,555 using in the range of 130–770 nm and ICP-AES analyzer (Varian, Vista-pro) was used for metal leaching of the sample in the course of recycling.

2.3. Preparation of catalyst

Graphene oxide (GO) was synthesized using a literature method and identified by FT-IR, Powder XRD, and SEM [44]. Then, a tri-component catalyst was synthesized with GO, reduced $H_4SiW_{12}O_{40}$ (SiW_{12}), and Fe_3O_4 nanoparticles.

2.3.1. Synthesis of $Fe_3O_4/SiW_{12}/GO$ composite

An aqueous solution of SiW_{12} (0.5 mmol, 10 mL) was adjusted to the pH = 1.18, and 1 mL of isopropanol was added to it; then the mixture solution was reduced photochemically with a UV light source (500 W Hg lamp) until the color of the solution become blue–black (approximate time = 30 min). The solution of reduced SiW_{12} was then mixed with GO (10 mL and 8 mg mL^{-1}) and Fe_3O_4 (0.5 mM) at room temperature in an ultrasonic bath. After 120 min of reaction, the tricomponent composites were assembled. The samples were then centrifuged and washed three times with pure water.

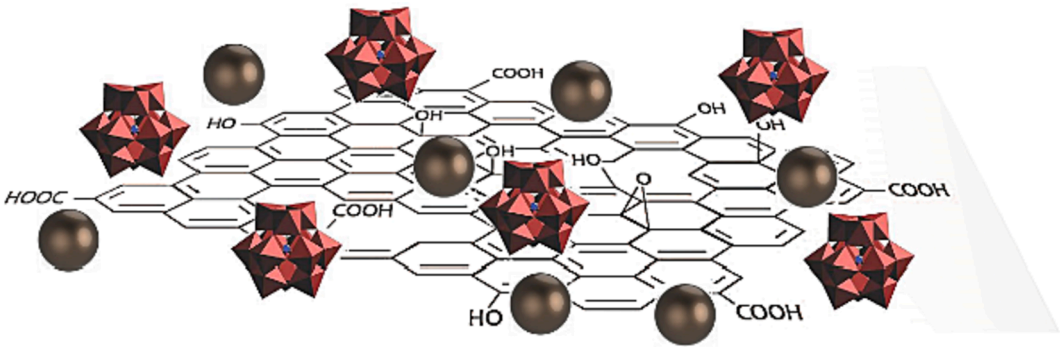

Fig. 1. Chemical structure of $Fe_3O_4/SiW_{12}/GO$ tricomponent catalyst with the representation of SiW_{12} (red polyhedral representation), Fe_3O_4 (grey mill representation), and GO. ((Colour online.))

Yield: 0.26 g (13 % based on W). FT-IR (KBr pellet, cm^{-1}): 3272, 3184, 1627, 1510, 1231, 1081, 971, 924, 794, 746, 591, 544.

2.4. Typical method for the catalytic oxidation of sulfides to sulfoxides

In a glass tube, a mixture of sulfide (1 mmol) and H_2O_2 30 % (2.0 equiv., 0.83 g) was prepared, and $Fe_3O_4/SiW_{12}/GO$ as a catalyst (10 mg) was added and stirred at r.t. As soon as the oxidation process was finished after the time had passed (checking the process with TLC (*n*-hexane/EtOAc:10/1)), $Fe_3O_4/SiW_{12}/GO$ was magnetically separated, and the reaction mixture with diethyl ether was washed (3 * 8 mL) and decanted. Finally, the combined organic layers were dehydrated by Na_2SO_4, and evaporated to give the products 70–98 % yields.

3. Result and discussion

3.1. Catalyst characterization

The tricomponent $Fe_3O_4/SiW_{12}/GO$ composite was synthesized by simple reaction using ultrasound-assisted co-precipitation synthesis method (Fig. 1). The introduction of the GO support during synthesis into the composite can effectively increase the specific surface area of the composite for the dispersion of Fe_3O_4 nanoparticles and SiW_{12} species. It is worth mentioning that electrostatic interaction between negatively charged reduced SiW_{12} prevents Fe_3O_4 NPs from aggregating [45,46].

The scanning Electron Microscopy (SEM) and transmission electron microscopy (TEM) were employed to ascertain the structure and morphology of the GO (smooth surface), SiW_{12} (cubic or rod-like morphology), Fe_3O_4 (regular cubic shape) [47] and $Fe_3O_4/SiW_{12}/GO$ composite (contains both cubic and rod-like components on the smooth surface) (Fig. S1a).

In situ EDX analysis (Fig. S2) displayed that solid tungsten and carbon peaks exist, accompanied by Fe peaks, confirming the existence of all three components in this composite. These results are consistent with the SEM and TEM observations (Fig. S1a and 2b).

The actual Fe_3O_4 and SiW_{12} loading of the composite were determined by inductively coupled plasma-mass spectroscopy (ICP-MS) which indicated 16 wt% for Fe and 26 wt% for SiW_{12} (Si (0.28 wt%) and W (16.15 wt%)).

To analyze the surface area of $Fe_3O_4/SiW_{12}/GO$ composite, the N_2 sorption isotherm was used at 77 K (Fig. S3). The calculated Brunanur-Emmett-Teller (BET) surface area for $Fe_3O_4/SiW_{12}/GO$ is 92.27 m^2/g [48]. Also, the total pore volume of $Fe_3O_4/SiW_{12}/GO$ obtained from N_2 isotherms ($P/P_0 = 0.95$) is 0.13 $cm^3\ g^{-1}$ and its mean pore diameter is 5.67 nm which confirms the mesoporous nature of composite.

The powder XRD pattern of Fe_3O_4, SiW_{12}, GO, and the $Fe_3O_4/SiW_{12}/GO$ composite are displayed in Fig. S4. As shown, the peak at $2\theta = 9.8^\circ$ corresponding to the C (0 0 2) of GO (represented sharp diffraction peak at an interlayer spacing of 0.790 nm) [37]. The complete oxidation of G is proven by the absence of any peak at a 2θ value of 26.5°. In addition, the $Fe_3O_4/SiW_{12}/GO$ composite showed diffraction peaks for the Fe_3O_4, SiW_{12}, and GO (the observed characteristic peaks at 36°, 8°, and 11° for 2θ value), which revealed the formation of tricomponent composite.

FT-IR spectra to analyze the chemical structures of the $Fe_3O_4/SiW_{12}/GO$ composite were recorded. Also, the IR spectra of the composite present a similar vibration pattern with the Fe_3O_4, SiW_{12}, and GO, confirming the presence of all moieties in it (Fig. 2). Briefly, the characteristic bands are attributed to the vibration of SiW_{12} in the range of 600–1100 cm^{-1}, and as it can be seen in the spectrum of SiW_{12} strong bands for W–O_c, W–O_t, W–O_b and Si–O stretching vibrations are around 801, 875, 970, and 921 cm^{-1}, respectively. In addition, the bands at 1221, 1436, 1520, and 1647 cm^{-1} region are assigned to the stretching vibration of C═C and C═O bonds in GO. Also, the vibration band of carboxylic groups on GO are at 1710 cm^{-1} shifted to 1627 cm^{-1} in the composite. This indicates that strong hydrogen bonds between the

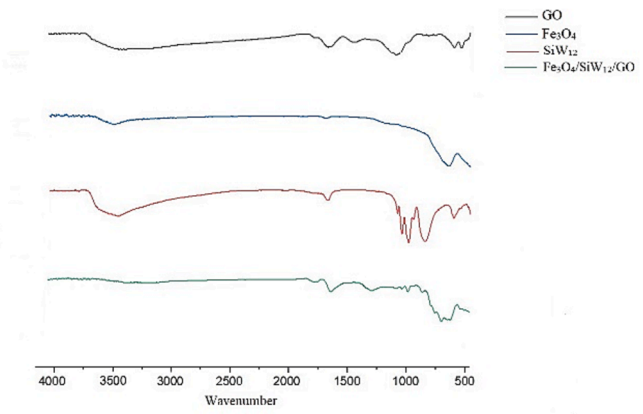

Fig. 2. FTIR spectra of the SiW_{12}, GO, Fe_3O_4, and prepared $Fe_3O_4/SiW_{12}/GO$ composite.

oxygen atoms of SiW_{12} and the hydroxyl groups on the carboxylic acids are formed. In addition, the characteristic peak was derived from the Fe − O − Fe of Fe_3O_4 at wavelength of 580 cm^{-1}. Compared with the characteristic bands of Fe_3O_4, SiW_{12}, and GO, $Fe_3O_4/SiW_{12}/GO$ composite contained all three characteristic absorption peaks and confirmed that our composite appropriately synthesized.

A vibrating sample magnetometer (VSM) was carried out to study the magnetic properties of the $Fe_3O_4/SiW_{12}/GO$ composite at room temperature. As displayed in Fig. 3, the maximum saturation magnetization intensity value of the $Fe_3O_4/SiW_{12}/GO$ composite was 43 emu/g, despite a few declines in comparison with unfunctionalized Fe_3O_4 (70 emu/g) due to the introduction of non-magnetic GO and SiW_{12} components, which further confirmed the successful formation of $Fe_3O_4/SiW_{12}/GO$ composite.

3.2. Catalytic activity

To explore the extended capabilities of the nanocatalyst, we conducted investigations on the catalytic activity of $Fe_3O_4/SiW_{12}/GO$ in the selective oxidation of sulfides. As a starting point, we examined the oxidation of methyl phenyl sulfide (MPS) using aqueous hydrogen peroxide (30 %) without the addition of other solvents (SF) and at room temperature conditions (rt) as a model reaction. In the absence of a catalyst, only 45 % of the product was obtained after 12 h of reaction time (Table 1, entry 1), as expected. To enhance the efficiency, we performed another reaction using MPS (1 mmol) in the presence of $Fe_3O_4/SiW_{12}/GO$ (10 mg) and H_2O_2 (2 eq.) at rt. This resulted in a methyl phenyl sulfoxide yield of 80 %, confirming the effective presence of the catalyst (Table 1, entry 2).

To gain further insights into this catalytic system and elucidate the active site responsible for MPS oxidation in $Fe_3O_4/SiW_{12}/GO$, we investigated several catalysts including raw Fe_3O_4, SiW_{12}, and GO (Table 1, entries 9–13). The obtained results, along with the analysis conducted, indicate that the presence of an active intermediate containing sulfur and oxygen in H_2O_2 can promote the reaction. Fig. 4 illustrates a possible mechanism for the catalytic oxidation of sulfide over the $Fe_3O_4/SiW_{12}/GO$ composite. Initially, H_2O_2 can bind to $Fe_3O_4/SiW_{12}/GO$ composite, forming an active electrophilic peroxide intermediate. Subsequently, this peroxide- $Fe_3O_4/SiW_{12}/GO$ intermediate can undergo a nucleophilic attack by the -S atom of the sulfide, leading to the reduction of $Fe_3O_4/SiW_{12}/GO$ back to its original state for subsequent runs, with the release of one mole of water. It is worth mentioning that GO and SiW_{12} play crucial roles in the development of metal-peroxide species and activation of H_2O_2 molecules. Similar mechanisms have been reported in recent literature for this reaction [49,50].

The results of the oxidation reaction of MPS in the presence of SiW_{12},

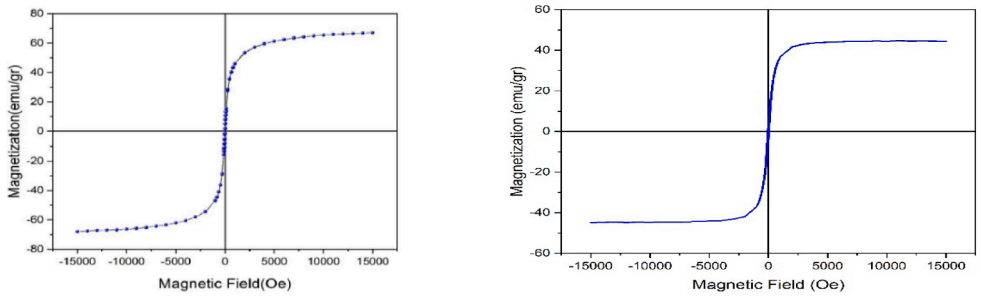

Fig. 3. Magnetic curves of (left) Fe_3O_4 and (right) Fe_3O_4/SiW_{12}/GO composite.

Table 1
Optimization of the reaction parameters and comparison of the catalytic performance of Fe_3O_4/SiW_{12}/GO with control catalysts in the oxidation of MPS.[a]

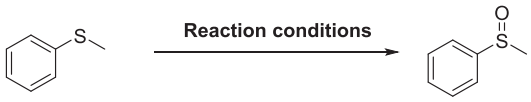

Entry	Catalyst (mg)	Conditions Oxidant (Equiv.)/ Solvent/ Temperature	Time (min)	Yield (%)
1	Fe_3O_4/SiW_{12}/GO (None)	H_2O_2 (2)/ SF/ rt	720	45
2	Fe_3O_4/SiW_{12}/GO (10)	H_2O_2 (2)/ SF/ rt	30	80
3	Fe_3O_4/SiW_{12}/GO (15)	H_2O_2 (2)/ SF/ rt	30	98
4	Fe_3O_4/SiW_{12}/GO (20)	H_2O_2 (2)/ SF/ rt	30	95
5	Fe_3O_4/SiW_{12}/GO (15)	H_2O_2 (1)/ SF/ rt	30	65
6	Fe_3O_4/SiW_{12}/GO (15)	H_2O_2 (1.5)/ SF/ rt	30	75
7	Fe_3O_4/SiW_{12}/GO (15)	H_2O_2 (None)/ SF/ rt	30	40
8	Fe_3O_4/SiW_{12}/GO (15)	O_2 / SF/ rt	30	55
9	Fe_3O_4 (15)	H_2O_2 (2)/ SF/ rt	30	30
10	GO (15)	H_2O_2 (2)/ SF/ rt	30	45
11	Fe_3O_4/SiW_{12} (15)	H_2O_2 (2)/ SF/ rt	30	70
12	SiW_{12}/GO (15)	H_2O_2 (2)/ SF/ rt	30	80
13	Fe_3O_4/GO (15)	H_2O_2 (2)/ SF/ rt	30	45
14	Fe_3O_4/SiW_{12}/GO (15)	H_2O_2 (2)/ EtOH/ rt	30	85
15	Fe_3O_4/SiW_{12}/GO (15)	H_2O_2 (2)/ H_2O/ rt	30	70
16	Fe_3O_4/SiW_{12}/GO (15)	H_2O_2 (2)/ CH_3Cl/ rt	30	Trace

[a] MPS (1 mmol) with one-drop MeOH.

GO, and raw Fe_3O_4 nanoparticles confirm that they are active surface generators but not sufficient catalysts (Table 1, entry 2). SiW_{12} acted as a relatively effective catalyst, but its isolation and recovery from the reaction mixture is challenging. Immobilizing it on graphene oxide and magnetic nanoparticles not only facilitated recovery but also significantly enhanced catalytic activity, possibly due to the synergistic effect between GO, SiW_{12}, and Fe_3O_4 (Table 1, entries 9–13). It is worth mentioning that among the compounds used, GO and SiW_{12} can interact effectively with hydrogen peroxide due to the abundance of oxygen on their surface, making them successful in creating an intermediate. Optimization of reaction conditions was conducted by varying the amounts of catalyst and oxidant in MPS oxidation under SF and rt conditions (Table 1, entries 1–4). Based on the catalyst loading levels, using 15 mg Fe_3O_4/SiW_{12}/GO yielded the best results, while higher and lower amounts were not suitable (Table 1, entry 3). Variation in the

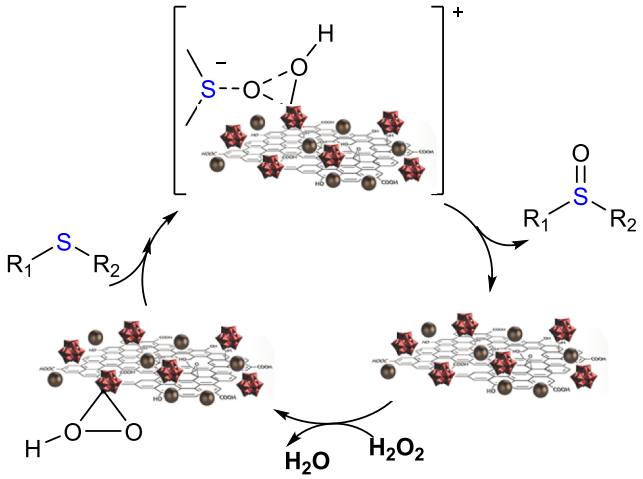

Fig. 4. A schematic possible mechanism for the oxidation of sulfide catalyzed by Fe_3O_4/SiW_{12}/GO and H_2O_2.

H_2O_2 amount indicated that 2.0 equivalents of H_2O_2 is optimal (Table 1, entries 3 and 5–7).

MPS was also oxidized with H_2O_2 on Fe_3O_4/SiW_{12}/GO in different solvents (2.5 mL). The results showed that no additional solvent was associated with better results (Table 1, entries 3 and 14–16). Additionally, using peroxide to complete the oxidation reaction was more crucial than under aerobic conditions (Table 1, entry 8).

The oxidation of different sulfides under the optimal conditions revealed that the Fe_3O_4/SiW_{12}/GO catalyst was effective for both aromatic and aliphatic sulfides (Table 2).

In the following, the findings of this investigations on the Fe_3O_4/SiW_{12}/GO catalyst with other recent reports on sulfide oxidation to sulfoxide were compared (Table 3, entries 1–6). The results demonstrate that this catalyst achieves better sulfide conversion under more favorable reaction conditions and shorter reaction times. Notably, the Fe_3O_4/SiW_{12}/GO composite offers the advantage of easy separation and high stability. The unique structure of SiW_{12}, which is well-stabilized on the surface of GO, contributes to the excellent performance of this heterogeneous catalyst.

Furthermore, the recyclability of Fe_3O_4/SiW_{12}/GO by conducting the model reaction under optimal conditions evaluated. After completion of the reaction, the mixture is washed with Et_2O to remove impurities. The Fe_3O_4/SiW_{12}/GO catalyst is then separated using a magnet, dried in air, and reutilized in the model reaction. Fig. 5 illustrates that the Fe_3O_4/SiW_{12}/GO catalyst can be successfully reused up to six times without significant loss of activity.

4. Conclusion

In conclusion, we have developed a sonochemical method for

Table 2
Synthesis of sulfoxides by the oxidation of sulfides over $Fe_3O_4/SiW_{12}/GO$ using H_2O_2 under SF at rt.[a]

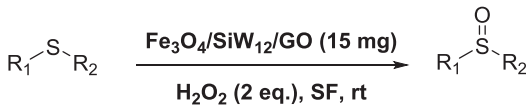

Entry	R^1	R^2	Time (min)	Yield (%)[b]	Conversion (%)	TON[c]	TOF[d] (min^{-1})	Selectivity (%)
1	C_6H_5	Me	30	98	98	0.74	0.024	100
2	C_6H_5	Et	45	85	90	0.64	0.014	100
3	C_6H_5	C_6H_5	75	77	80	0.58	0.007	100
4	*p*-MeC_6H_4	Me	60	85	90	0.64	0.01	100
5	*p*-BrC_6H_4	Me	90	70	75	0.53	0.005	100
6	*p*-$O_2NC_6H_4$	Me	60	83	85	0.63	0.01	100
7	*p*-HOC_6H_4	Me	70	88	88	0.67	0.009	100
8	Me	Me	80	72	75	0.54	0.006	100
9	Me	Et	100	70	70	0.53	0.005	100
10	Me	H	45	87	90	0.66	0.014	100

[a]Reaction condition: a mixture of sulfide (1 mmol), H_2O_2 (2 eq.) and $Fe_3O_4/SiW_{12}/GO$ (15 mg) was stirred without any solvent.
[b]Isolated yields.
[c]TON = Conversion (%)/Catalyst amount (mol% of W).
[d]TOF = TON / Time (min).

Table 3
Comparison of catalytic activity of $Fe_3O_4/SiW_{12}/GO$ with other reported catalysts for the reduction.

Entry	Catalyst (Amount)	Conditions Oxidant	Solvent	Temp. or UV	Time (min)	Conversion (%)	Ref.
1	Mo_6W_6@EDMG (7 mg)	H_2O_2 (1.5 mmol)	EtOH	400 W lamp	120	88	[51]
2	MNP@TA-IL/W (0.4 mol%)	H_2O_2 (1.5 e.q)	H_2O	rt	60	98	[52]
3	Fe_3O_4@S-ABENZ@VO (5 mg)	H_2O_2 (16 mmol)	SF	rt	80	98	[53]
4	VO(BINE)@Fe_3O_4 (30 mg)	H_2O_2 (2 mmol)	SF	rt	5	96	[18]
5	PAMAM-G1-PMo (50 mg)	H_2O_2 (0.55 mmol)	MeOH	rt	240	88	[54]
6	$Fe_3O_4/SiW_{12}/GO$ (15 mg)	H_2O_2 (1.5 mmol)	SF	rt	30	98	This work

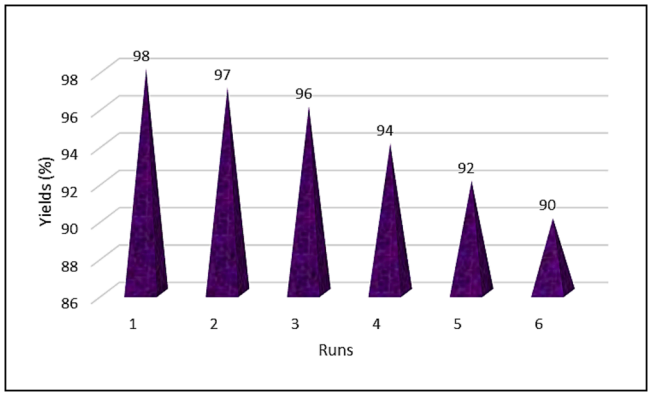

Fig. 5. Reusability of $Fe_3O_4/SiW_{12}/GO$ in the oxidation of MPS by H_2O_2.

preparing a three-component composite catalyst, $Fe_3O_4/SiW_{12}/GO$, for efficient sulfide oxidation. This catalyst offers numerous advantages compared to previous solid supports, including enhanced activity, stability, and retrievability. The incorporation of GO to stabilize SiW_{12} and Fe_3O_4 nanoparticles not only improves the catalytic performance but also facilitates its recyclability. Overall, $Fe_3O_4/SiW_{12}/GO$ demonstrates excellent potential for the oxidation of various sulfides to sulfoxides, providing a green, economical, and time-efficient approach for their synthesis. Given the wide application of sulfides in industries such as agriculture and pharmaceuticals, this protocol holds significant promise for sustainable and environmentally friendly production.

Competing interests

The authors declare no competing interests.

CRediT authorship contribution statement

Masoume Malmir: Methodology, Formal analysis, Data curation, Software, Validation, Writing – original draft, Writing – review & editing. **Majid M. Heravi:** Supervision, Project administration, Visualization, Writing – review & editing. **Zahra Yekke-Ghasemi:** Methodology, Formal analysis, Data curation, Software, Validation, Writing – original draft, Writing – review & editing. **Masoud Mirzaei:** Supervision, Project administration, Visualization, Writing – review & editing.

Declaration of Competing Interest

The authors declare that they have no known competing financial interests or personal relationships that could have appeared to influence the work reported in this paper.

Data availability

All data related to the project is presented in the article.

Acknowledgment

The Alzahra University, Tehran, Iran and Ferdowsi University of Mashhad, Mashhad, Iran financially support this project and all authors appreciate them.

Appendix A. Supplementary data

Supplementary data to this article can be found online at https://doi.org/10.1016/j.poly.2023.116729.

References

[1] M. Malmir, M.M. Heravi, Z. Yekke-Ghasemi, M. Mirzaei, Incorporating heterogeneous lacunary Keggin anions as efficient catalysts for solvent-free cyanosilylation of aldehydes and ketones, Sci. Rep. 12 (2022) 11573, https://doi.org/10.1038/s41598-022-15831-1.

[2] M. Bazargan, M. Mirzaei, A. Amiri, J.T. Mague, Opioid Drug Detection in Hair Samples Using Polyoxometalate-Based Frameworks, Inorg. Chem. 62 (2023) 56–65, https://doi.org/10.1021/acs.inorgchem.2c02658.

[3] C. Zhou, S. Li, W. Zhu, H. Pang, H. Ma, A sensor of a polyoxometalate and Au-Pd alloy for simultaneously detection of dopamine and ascorbic acid, Electrochim. Acta 113 (2013) 454–463, https://doi.org/10.1016/j.electacta.2013.09.109.

[4] M. Babaei Zarch, M. Mirzaei, M. Bazargan, S.K. Gupta, F. Meyer, J.T. Mague, Single-molecule magnets within polyoxometalate-based frameworks, Dalton Trans. 50 (2021) 15047–15056, https://doi.org/10.1039/D1DT01708J.

[5] M. Arefian, M. Mirzaei, H. Eshtiagh-Hosseini, A. Frontera, A survey of the different roles of polyoxometalates in their interaction with amino acids, peptides and proteins, Dalton Trans. 46 (2017) 6812–6829, https://doi.org/10.1039/C7DT00894E.

[6] H. Wang, S. Hamanaka, Y. Nishimoto, S. Irle, T. Yokoyama, H. Yoshikawa, K. Awaga, In Operando X-ray Absorption Fine Structure Studies of Polyoxometalate Molecular Cluster Batteries: Polyoxometalates as Electron Sponges, J. Am. Chem. Soc. 134 (2012) 4918–4924, https://doi.org/10.1021/ja2117206.

[7] C. Jia, J. Zhao, L. Lei, X. Kang, R. Lu, C. Chen, S. Li, Y. Zhao, Q. Yang, Z. Chen, Novel magnetically separable anhydride-functionalized Fe_3O_4@SiO_2@PEI-NTDA nanoparticles as effective adsorbents: synthesis, stability and recyclable adsorption performance for heavy metal ions, RSC Adv. 9 (2019) 9533–9545, https://doi.org/10.1039/C8RA10310K.

[8] A. Khodadadi Dizaji, H.R. Mortaheb, B. Mokhtarani, Preparation of supported catalyst by adsorption of polyoxometalate on graphene oxide/reduced graphene oxide, Mater. Chem. Phys. 199 (2017) 424–434, https://doi.org/10.1016/j.matchemphys.2017.07.016.

[9] K. Darvishi, K. Amani, M. Rezaei, Preparation, characterization and heterogeneous catalytic applications of GO/Fe_3O_4/HPW nanocomposite in chemoselective and green oxidation of alcohols with aqueous H_2O_2, Appl. Organomet. Chem. 32 (2018) e4323.

[10] F. Cavani, J.H. Teles, Sustainability in Catalytic Oxidation: An Alternative Approach or a Structural Evolution? Chem. Sus. Chem. 2 (2009) 508–534, https://doi.org/10.1002/cssc.200900020.

[11] J.M. Campos-Martin, G. Blanco-Brieva, J.L.G. Fierro, Hydrogen Peroxide Synthesis: An Outlook beyond the Anthraquinone Process, Angew. Chem. Int. Ed. 45 (2006) 6962–6984, https://doi.org/10.1002/anie.200503779.

[12] F. Faccioli, M. Bauer, D. Pedron, A. Sorarù, M. Carraro, S. Gross, Hydrolytic Stability and Hydrogen Peroxide Activation of Zirconium-Based Oxoclusters, Eur. J. Inorg. Chem. 2015 (2015) 210–225, https://doi.org/10.1002/ejic.201402767.

[13] M. Hajjami, L. Shiri, A. Jahanbakhshi, Zirconium oxide complex-functionalized MCM-41 nanostructure: an efficient and reusable mesoporous catalyst for oxidation of sulfides and oxidative coupling of thiols using hydrogen peroxide, Appl. Organomet. Chem. 29 (2015) 668–673, https://doi.org/10.1002/aoc.3348.

[14] T. Tamoradi, A. Ghorbani-Choghamarani, M. Ghadermazi, Synthesis of new zirconium complex supported on MCM-41 and its application as an efficient catalyst for synthesis of sulfides and the oxidation of sulfur containing compounds, Appl. Organomet. Chem. 32 (2018) e4340.

[15] J. Wang, Y. Zhou, M. Zeng, Y. Zhao, X. Zuo, F. Meng, F. Lv, Y. Lu, Zr(IV)-based metal-organic framework nanocomposites with enhanced peroxidase-like activity as a colorimetric sensing platform for sensitive detection of hydrogen peroxide and phenol, Environ. Res. 203 (2022), 111818, https://doi.org/10.1016/j.envres.2021.111818.

[16] P.-Y. Zhang, Y. Wang, L.-Y. Yao, G.-Y. Yang, Hepta-Zr-Incorporated Polyoxometalate Assembly, Inorg. Chem. 61 (2022) 10410–10416, https://doi.org/10.1021/acs.inorgchem.2c01124.

[17] [17] N. V. Maksimchuk, V.Y. Evtushok, O. V. Zalomaeva, G.M. Maksimov, I.D. Ivanchikova, Y.A. Chesalov, I. V. Eltsov, P.A. Abramov, T.S. Glazneva, V. V. Yanshole, O.A. Kholdeeva, R.J. Errington, A. Solé-Daura, J.M. Poblet, J.J. Carbó, Activation of H_2O_2 over Zr(IV). Insights from Model Studies on Zr-Monosubstituted Lindqvist Tungstates, ACS Catal. 11 (2021) 10589–10603. https://doi.org/10.1021/acscatal.1c02485.

[18] H. Veisi, A. Rashtiani, A. Rostami, M. Shirinbayan, S. Hemmati, Chemo-selective oxidation of sulfide to sulfoxides with H_2O_2 catalyzed by oxo-vanadium/Schiff-base complex immobilized on modified magnetic Fe_3O_4 nanoparticles as a heterogeneous and recyclable nanocatalyst, Polyhedron 157 (2019) 358–366, https://doi.org/10.1016/j.poly.2018.09.034.

[19] I.D. Ivanchikova, N.V. Maksimchuk, I.Y. Skobelev, V.V. Kaichev, O.A. Kholdeeva, Mesoporous niobium-silicates prepared by evaporation-induced self-assembly as catalysts for selective oxidations with aqueous H_2O_2, J. Catal. 332 (2015) 138–148, https://doi.org/10.1016/j.jcat.2015.10.003.

[20] N.E. Thornburg, A.B. Thompson, J.M. Notestein, Periodic Trends in Highly Dispersed Groups IV and V Supported Metal Oxide Catalysts for Alkene Epoxidation with H_2O_2, ACS Catal. 5 (2015) 5077–5088, https://doi.org/10.1021/acscatal.5b01105.

[21] M.S.S. Adam, A. Taha, M.M. Mostafa, F. Ullah, M.M. Makhlouf, ZnO–TiO2 Nanoparticles Coated by the Dioxomolybdenum (VI) bis -Schiff Base Complex for Catalytic Oxidation of Sulfides, ACS Appl. Nano Mater. 6 (2023) 8515–8528, https://doi.org/10.1021/acsanm.3c00885.

[22] B. Li, A.-H. Liu, L.-N. He, Z.-Z. Yang, J. Gao, K.-H. Chen, Iron-catalyzed selective oxidation of sulfides to sulfoxides with the polyethylene glycol/O_2 system, Green Chem. 14 (2012) 130–135, https://doi.org/10.1039/C1GC15821J.

[23] M.S.S. Adam, M.A. Al-Omair, Nanocomposite-based inorganic-organocatalyst Cu (II) complex and SiO2 - and Fe3O4 nanoparticles as low-cost and efficient catalysts for aniline and 2-aminopyridine oxidation, Appl. Organomet. Chem. 34 (2020), https://doi.org/10.1002/aoc.5999.

[24] N. Moeini, M. Ghadermazi, S. Molaei, Synthesis and characterization of magnetic Fe_3O_4@Creatinine@Zr nanoparticles as novel catalyst for the synthesis of 5-substituted 1H-tetrazoles in water and the selective oxidation of sulfides with classical and ultrasonic methods, J. Mol. Struct. 1251 (2022), 131982, https://doi.org/10.1016/j.molstruc.2021.131982.

[25] G. Abdi, A. Alizadeh, M.M. Khodaei, Highly carboxyl-decorated graphene oxide sheets as metal-free catalytic system for chemoselective oxidation of sulfides to sulfones, Mater. Chem. Phys. 201 (2017) 323–330, https://doi.org/10.1016/j.matchemphys.2017.08.062.

[26] Johannes Karl Fink, No TitleHigh Performance Polymers, William Andrew Publishing, Norwich, NY, 2008, pp. 1–68.

[27] M. Ghanbari Kermanshahi, K. Bahrami, Fe_3O_4@BNPs@SiO_2–SO_3 H as a highly chemoselective heterogeneous magnetic nanocatalyst for the oxidation of sulfides to sulfoxides or sulfones, RSC Adv. 9 (2019) 36103–36112, https://doi.org/10.1039/C9RA06221A.

[28] S. Sadjadi, G. Lazzara, M. Malmir, M.M. Heravi, Pd nanoparticles immobilized on the poly-dopamine decorated halloysite nanotubes hybridized with N-doped porous carbon monolayer: A versatile catalyst for promoting Pd catalyzed reactions, J. Catal. 366 (2018) 245–257, https://doi.org/10.1016/j.jcat.2018.08.013.

[29] S. Sadjadi, M. Malmir, G. Lazzara, G. Cavallaro, M.M. Heravi, Preparation of palladated porous nitrogen-doped carbon using halloysite as porogen: disclosing its utility as a hydrogenation catalyst, Sci. Rep. 10 (2020) 2039, https://doi.org/10.1038/s41598-020-59003-5.

[30] G. Jahani, M. Malmir, M.M. Heravi, Catalytic Oxidation of Alcohols over a Nitrogen- and Sulfur-Doped Graphitic Carbon Dot-Modified Magnetic Nanocomposite, Ind. Eng. Chem. Res. 61 (2022) 2010–2022, https://doi.org/10.1021/acs.iecr.1c04198.

[31] M.B. Bisafar, M. Malmir, M.M. Heravi, Highly selective reduction of nitro compounds catalyzed by MOF-derived glucose stabilized Fe3O4 under mild conditions, J. Chem. Technol. Biotechnol. (2023), https://doi.org/10.1002/jctb.7500.

[32] Z. Yekke-Ghasemi, M.M. Heravi, M. Malmir, M. Mirzaei, Efficient oxidation of sulfides to sulfoxides catalyzed by heterogeneous Zr-containing polyoxometalate grafted on graphene oxide, Sci. Rep. 13 (2023) 16752, https://doi.org/10.1038/s41598-023-43985-z.

[33] M. Malmir, M.M. Heravi, G. Jahani, An efficient catalytic reduction of nitroarenes over metal-organic framework-derived magnetic graphitic carbon nitride nanosheet, Appl. Organomet. Chem. (2023), https://doi.org/10.1002/aoc.7277.

[34] M.M. Heravi, L. Mohammadkhani, Synthesis of various N-heterocycles using the four-component Ugi reaction, in: 2020: pp. 351–403. https://doi.org/10.1016/bs.aihch.2019.04.001.

[35] M.M. Heravi, B. Talaei, Ketenes as Privileged Synthons in the Synthesis of Heterocyclic Compounds Part 3, in: 2016: pp. 195–291. https://doi.org/10.1016/bs.aihch.2015.10.007.

[36] M.M. Heravi, B. Talaei, Diketene as Privileged Synthon in the Syntheses of Heterocycles Part 1, in: 2017: pp. 43–114. https://doi.org/10.1016/bs.aihch.2016.10.003.

[37] Z. Amiri, M. Malmir, T. Hosseinnejad, K. Kafshdarzadeh, M.M. Heravi, Combined experimental and computational study on Ag-NPs immobilized on rod-like hydroxyapatite for promoting Hantzsch reaction, Mol. Catal. 524 (2022), 112319, https://doi.org/10.1016/j.mcat.2022.112319.

[38] M. Malmir, M.M. Heravi, Z. Amiri, K. Kafshdarzadeh, Magnetic composite of γ-Fe2O3 hollow sphere and palladium doped nitrogen-rich mesoporous carbon as a recoverable catalyst for C-C coupling reactions, Sci. Rep. 11 (2021) 22409, https://doi.org/10.1038/s41598-021-99679-x.

[39] Z.N. Sisakhti, M. Malmir, M.B. Bisafar, M.M. Heravi, T. Hosseinnejad, Direction of theoretical and experimental investigation into the mechanism of n-HA/Si-PA-SC@Ag as a bio-based heterogeneous catalyst in the reduction reactions, Sci. Rep. 12 (2022) 21964, https://doi.org/10.1038/s41598-022-26200-3.

[40] K. Kafshdarzadeh, M. Malmir, Z. Amiri, M.M. Heravi, Ionic liquid-loaded triazine-based magnetic nanoparticles for promoting multicomponent reaction, Sci. Rep. 12 (2022) 22261, https://doi.org/10.1038/s41598-022-26235-6.
[41] Z. Besharati, M. Malmir, M.M. Heravi, Cu_2O NPs immobilized on Montmorilonite-K10 decorated by acidic-ionic liquid: An environmentally friendly, heterogeneous and recyclable catalyst for the synthesis of benzopyranopyrimidines, Inorg. Chem. Commun. 143 (2022), 109813, https://doi.org/10.1016/j.inoche.2022.109813.
[42] Z. Yekke-Ghasemi, M.M. Heravi, M. Malmir, G. Jahani, M.B. Bisafar, M. Mirzaei, Fabrication of heterogeneous-based lacunary polyoxometalates as efficient catalysts for the multicomponent and clean synthesis of pyrazolopyranopyrimidines, Inorg. Chem. Commun. 140 (2022), 109456, https://doi.org/10.1016/j.inoche.2022.109456.
[43] Z. Yekke-Ghasemi, M.M. Heravi, M. Malmir, M. Mirzaei, Monosubstituted Keggin as heterogeneous catalysts for solvent-free cyanosilylation of aldehydes and ketones, Catal. Commun. 171 (2022), 106499, https://doi.org/10.1016/j.catcom.2022.106499.
[44] M. Kigozi, R.K. Koech, O. Kingsley, I. Ojeaga, E. Tebandeke, G.N. Kasozi, A. P. Onwualu, Synthesis and characterization of graphene oxide from locally mined graphite flakes and its supercapacitor applications, Results Mater. 7 (2020), 100113, https://doi.org/10.1016/j.rinma.2020.100113.
[45] S. Li, X. Yu, G. Zhang, Y. Ma, J. Yao, B. Keita, N. Louis, H. Zhao, Green chemical decoration of multiwalled carbon nanotubes with polyoxometalate-encapsulated gold nanoparticles: visible light photocatalytic activities, J. Mater. Chem. 21 (2011) 2282–2287, https://doi.org/10.1039/C0JM02683B.
[46] R. Liu, S. Li, X. Yu, G. Zhang, S. Zhang, J. Yao, B. Keita, L. Nadjo, L. Zhi, Facile Synthesis of Au-Nanoparticle/Polyoxometalate/Graphene Tricomponent Nanohybrids: An Enzyme-Free Electrochemical Biosensor for Hydrogen Peroxide, Small. 8 (2012) 1398–1406, https://doi.org/10.1002/smll.201102298.
[47] H. Fatima, D.-W. Lee, H.J. Yun, K.-S. Kim, Shape-controlled synthesis of magnetic Fe_3O_4 nanoparticles with different iron precursors and capping agents, RSC Adv. 8 (2018) 22917–22923, https://doi.org/10.1039/C8RA02909A.
[48] X. Jing, Z. Li, W. Geng, H. Lv, Y. Chi, C. Hu, Polyoxometalate-modified reduced graphene oxide foam as a monolith reactor for efficient flow catalysis of epoxide ring-opening reactions, J. Mater. Chem. A 9 (2021) 8480–8488, https://doi.org/10.1039/D0TA11188K.
[49] T.-Y. Dang, R.-H. Li, H.-R. Tian, Q. Wang, Y. Lu, S.-X. Liu, Tandem-like vanadium cluster chains in a polyoxovanadate-based metal–organic framework for efficient catalytic oxidation of sulfides, Inorg. Chem. Front. 8 (2021) 4367–4375, https://doi.org/10.1039/D1QI00799H.
[50] H. Li, C. Lian, L. Chen, J. Zhao, G.-Y. Yang, Two unusual nanosized Nd3+ -substituted selenotungstate aggregates simultaneously comprising lacunary Keggin and Dawson polyoxotungstate segments, Nanoscale. 12 (2020) 16091–16101, https://doi.org/10.1039/D0NR04051G.
[51] H. Fakhri, A. Mahjoub, R. Nejat, A. Maridiroosi, Fabrication of molybdenum-substituted tungstophosphoric acid immobilized onto functionalized graphene oxide: Visible light-induced photocatalyst for selective oxidation of sulfides to sulfoxides, Inorg. Chem. Commun. 123 (2021), 108353, https://doi.org/10.1016/j.inoche.2020.108353.
[52] S.H. Hosseini, M. Tavakolizadeh, N. Zohreh, R. Soleyman, Green route for selective gram-scale oxidation of sulfides using tungstate/triazine-based ionic liquid immobilized on magnetic nanoparticles as a phase-transfer heterogeneous catalyst, Appl. Organomet. Chem. 32 (2018) e3953.
[53] S. Rezaei, A. Ghorbani-Choghamarani, R. Badri, A. Nikseresht, Fe_3O_4 @S-ABENZ@VO: Magnetically separable nanocatalyst for the efficient, selective and mild oxidation of sulfides and oxidative coupling of thiols, Appl. Organomet. Chem. 32 (2018) e3948.
[54] Q.-L. Tong, Z.-F. Fan, J.-W. Yang, Q. Li, Y.-X. Chen, M.-S. Cheng, Y. Liu, The Selective Oxidation of Sulfides to Sulfoxides or Sulfones with Hydrogen Peroxide Catalyzed by a Dendritic Phosphomolybdate Hybrid, Catalysts 9 (2019) 791, https://doi.org/10.3390/catal9100791.